THIN-FILM PERIPHERAL NERVE ELECTRODE

Tri-Annual Progress Report

Covering Period October 1, 1994 to January 31, 1995

CONTRACT NO. N44-NS-3-2367

by

S. F. Cogan
Y-P. Liu
Jurgen L. Holleck
EIC Laboratories, Inc.
111 Downey Street
Norwood, Massachusetts 02062

and
James D. Walter
Hines VA Hospital
Rehabilitation R&D Center
Hines, Illinois 60141

Prepared for

National Institutes of Health
National Institute of Neurological
Disorders and Stroke
Bethesda, Maryland 20892

June 13, 1995

Table Of Contents

List Of Figures

List Of Tables

1.0 BACKGROUND

A program to develop a functional neuromuscular system (FNS) capable of graded and stable activation of hand muscles for the restoration of grasp in quadriplegic individuals is being undertaken. The objective of the program is the development of a thin film neural cuff electrode and the demonstration of the efficacy of the electrode for grasp in an *in vivo* study using a raccoon model.

Specific features of the proposed electrode include:

- multiple, independently addressable charge injection sites that will facilitate implementation of established and emerging stimulation protocols such as anodal field steering and anodal blocking;
- leads and electrodes are vacuum deposited on a planar, monolithic fluorocarbon substrate that is flexible and avoids bulky interconnects in close proximity to the implantation site;
- charge injection electrodes of Pt or activated iridium oxide (AIROF), both of which are stable under the anticipated charge injection protocols;
- fluorocarbon substrates that can be thermoformed into a self-sizing cuff to allow a snug but elastic fit to the nerve.

The circumneural electrodes are fabricated by vacuum depositing metal films on thin sheets of fluorocarbon polymer and photolithographically patterning and the leads and charge injection sites. The patterned substrate is then thermally sealed with a second polymer layer to electronically isolate the leads from the physiological environment. The charge injection sites are exposed by a combination of photolithography and ion or plasma etching of vias through the polymer overlayer. Once all planar fabrication processes, i.e., photolithography, vacuum deposition, and etching have been completed, the electrode is cut out of the substrate and the desired cuff and lead geometries created by thermoforming.

An example of an electrode in planar geometry prior to thermoforming the cuff is shown in Figure 1. The leads and charge injection sites are patterned on a large polymer substrate with the leads extending to a bonding pad located several centimeters from the cuff. Four charge injection sites, designed to evaluate anodal steering, are shown on the cuff.

2.0 TECHNICAL PROGRESS

In the fourth reporting period, an extensive evaluation of the raccoon model and studies of selectivity with intramuscular electrodes and a 12 electrode cuff on the median nerve were conducted at the Hines V.A. Rehabilitation R&D Center. This work is detailed in Appendix I. Work on the development of thin film electrodes on FEP Teflon substrates has continued. The use of a spin coatable Teflon AF polymer as the inner insulating layer was abandoned due to the difficulty in obtaining adequate adhesion to the FEP Teflon. A silicone polymer, MED-6605 with primer SP-135, from NuSil Silicone Technology (Carpartina, CA), was evaluated as an

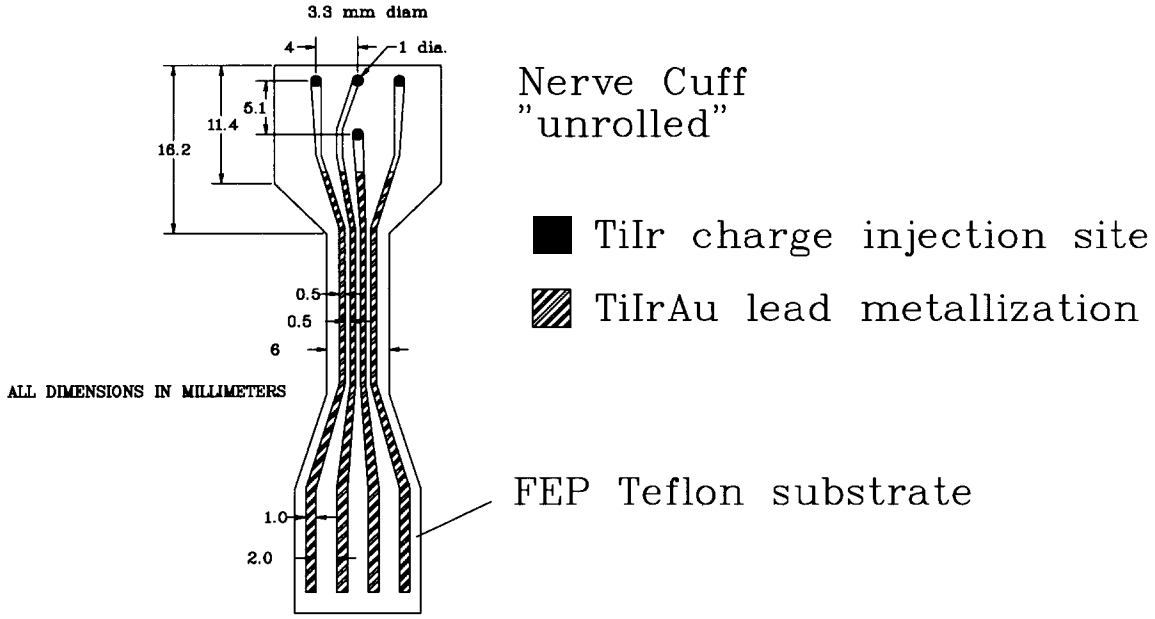

Figure 1. A circumneural cuff having four charge injection sites in a geometry suitable for evaluating anodal steering.

alternative. The silicone polymer was far more adherent than the Teflon AF and remained adherent throughout extensive *in vitro* electrochemical testing of the four-electrode cuff.

2.1 Cuff Fabrication

Four-electrode nerve cuffs on thermoformed FEP Teflon were fabricated and evaluated by *in vitro* electrochemical measurements. The charge injection sites on the cuffs were formed by sputtering a Ti/Ir bilayer. The Ti layer was sputtered with a -80 V substrate bias to improve adhesion to the Teflon. After Ir deposition the vacuum chamber was opened and the area around the charge injection sites masked with a thin glass cover slip. The remainder of the metallization, the interconnect and bond pads, were then coated with a sputtered Ti/Au bilayer to reduce interconnect resistance. The Au was further overcoated with a thin film of Ti to improve adhesion of the silicone polymer used as an insulator on the interior surface of the cuffs. The charge injection sites and bonding pads were masked with tape during the application of the silicone. Attempts at plasma or chemically etching the silicone to open vias to underlying electrodes or bonding pads were not successful and physical masking of these sites during spin coating of the silicone was required. The wrapped portion of the cuff electrodes was then formed by placing the cuffs in an aluminum mold and autoclaving at 135°C for 45 minutes.

2.2 *In vitro* Electrochemical Characterization

The electrochemical behavior at the electrode sites was evaluated by cyclic voltammetry and charge-injection in a two-buffer saline electrolyte. The electrolyte contained carbonate and

phosphate buffers in the same composition found in interstitial fluid (1); 137 mM NaCl, 29 mM $NaHCO_3$, 1.7 mM Na_2HP0_4 and 0.7 mM NaH_2PO_4 purged with a 5% CO_2/6% O_2/89% N_2 gas mixture to a pH of 7.4. Connection to the individual electrodes was made by attaching stainless steel wire to the bonding pads with electrically conductive epoxy. The electrochemical cell contained a saturated calomel reference electrode (SCE) for potential measurements and a Pt mesh counter electrode.

An initial cyclic voltammogram of a charge injection site is shown in Fig. 2. The electrode was cycled between limits of -0.6 and 0.8 V vs SCE at a sweep rate of 50 mV/s. The large currents on the cathodic sweep are associated with reduction of oxygen and water. After cycling for 40 minutes between these potential limits, activation of the electrode is observed as shown by the CV in Fig. 3. A distinct reduction-oxidation wave develops in the 0.0 V to 0.4 V potential range and the reduction at the negative potential limit is greatly reduced. After 100 minutes of cycling, shown in Fig. 4, the feature of the CV become similar to Ir wire electrodes activated in the same electrolyte.

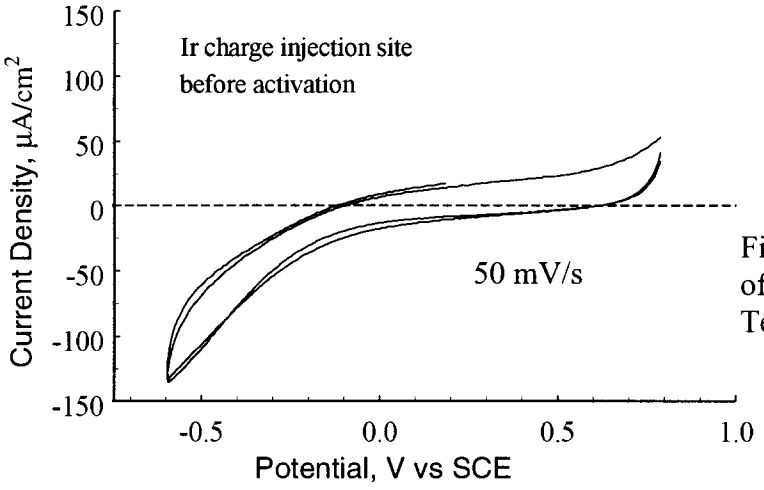

Figure 2. Initial cyclic voltammogram of an Ir charge injection site on a FEP Teflon cuff electrode.

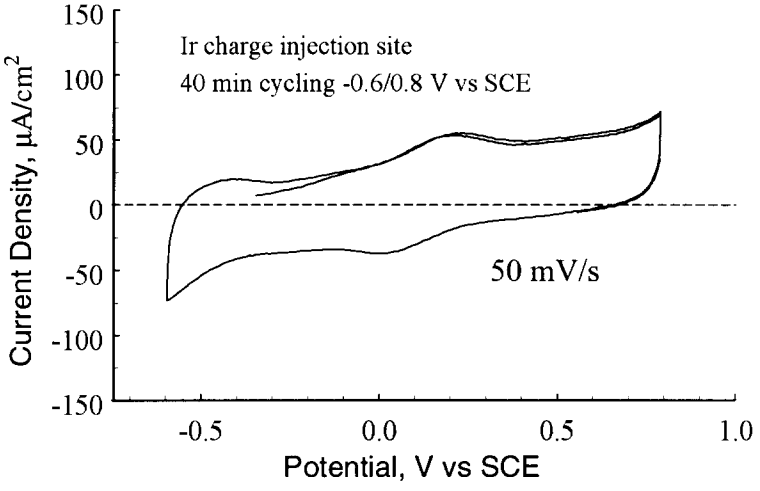

Figure 3. Cyclic voltammogram of a charge injection site after 40 minutes of cycling between -0.6 V and 0.8 V. Activation of the Ir is evident from the CV.

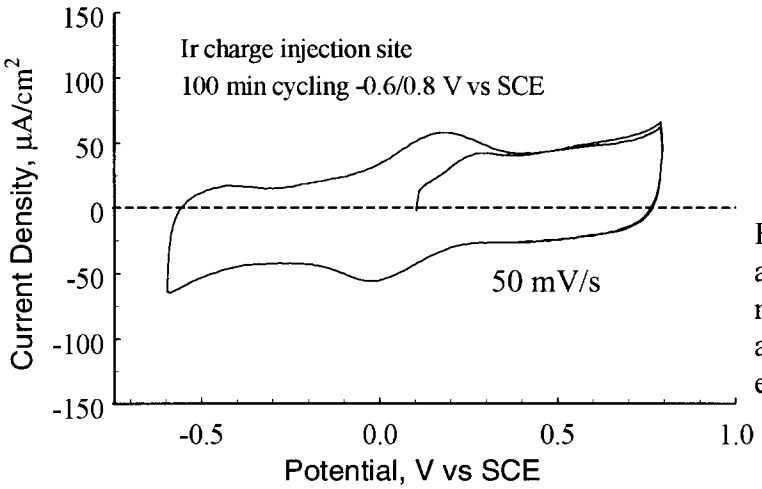

Figure 4. Cyclic voltammogram of a charge injection site after 100 minutes of cycling between -0.6 V and 0.8 V. Activation of the Ir is evident from the CV.

After 18 hr of continuous cycling, the charge capacity at a single electrode site had increased during a 50 mV/s CV to about 5 mC/cm^2. A CV of an electrode site with a capacity of 5.1 mC/cm^2 on the cathodic sweep is shown in Fig. 5. The "noisy" current response is due to the gas mixture bubbling into the electrolyte. The charge injection characteristics of the electrode were evaluated using monophasic, capacitively coupled pulses at a repetition rate of 60 pps and pulse width of 100 μs. The anodal and cathodal charge capacity, interpulse potential (IPP), access resistance (R_a), maximum current (I_{max}), and open-circuit potential after 2 minutes without pulsing (V_{oc}) are listed in Table 1. The maximum charge capacity is defined as that which produces a potential transient of -0.6 and 0.8 V vs SCE on cathodal and anodal pulsing, respectively.

Table 1. Charge injection characteristics of an Ir electrode site after 18 hours of potential cycling in PBS/CBS between -0.6 V and 0.8 V vs SCE.

Pulse Direction	Max. Current mA	Max. Charge μC/cm^2	IPP V vs SCE	Access Resistance Ω	V_{oc} V vs SCE
Anodal	7.6	97	0.05	87	0.08
Cathodal	8.6	110	0.04	74	0.05

The electrode was then deliberately activated by potential cycling at 50 mV/s between limits of -0.82 V and 0.96 V vs SCE. After activation, the cathodic charge capacity during cyclic voltammetry (-0.6 to 0.8 V vs SCE limits) doubles to ~10 mC/cm^2, as shown in Fig. 5. The corresponding charge capacity during pulsing, detailed in Table 2, increases to 190 μC/cm^2. This electrode was then pulsed continuously for 16 hr with 10 mA (130 μC/cm^2) cathodal pulses. The initial and final charge injection characteristics with the 10 mA pulses are listed in Table 3. The maximum cathodic potential excursion (E_{mc}), corrected for the access voltage, decreased from -0.380 V to -0.320 V during the pulsing. Comparison of the CV response after pulsing,

shown in Fig. 6, shows little change in electrode behavior from that prior to pulsing (Fig. 5), except for a modest increase in charge capacity..

Table 2. Charge injection characteristics of an Ir electrode site after 30 minutes of activation in PBS/CBS between -0.82 V and 0.96 V vs SCE.

Pulse Direction	Max. Current mA	Max. Charge $\mu C/cm^2$	IPP V vs SCE	Access Resistance Ω	V_{oc} V vs SCE
Anodal	15	191	0.07	75	0.08
Cathodal	14.8	189	0.06	70	0.08

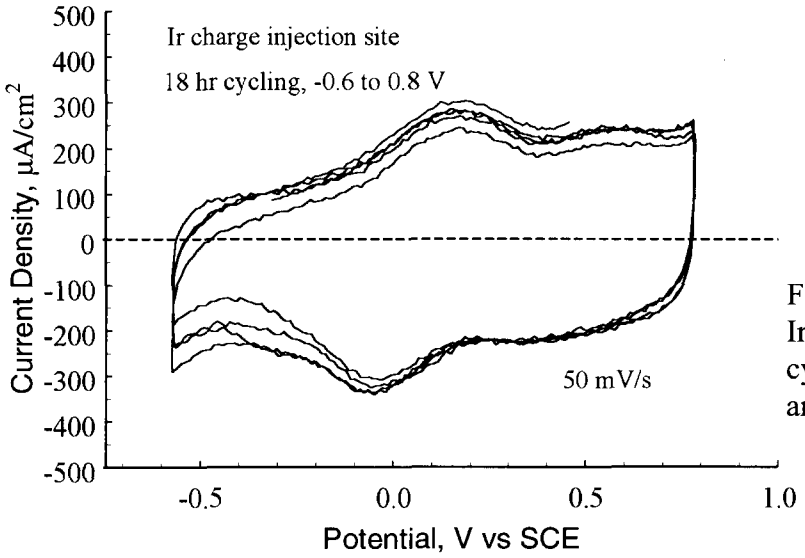

Figure 5. Cyclic voltammogram of Ir charge injection site after 18 hr cycling between limits of -0.6 V and 0.8 V vs SCE at 50 mV/s.

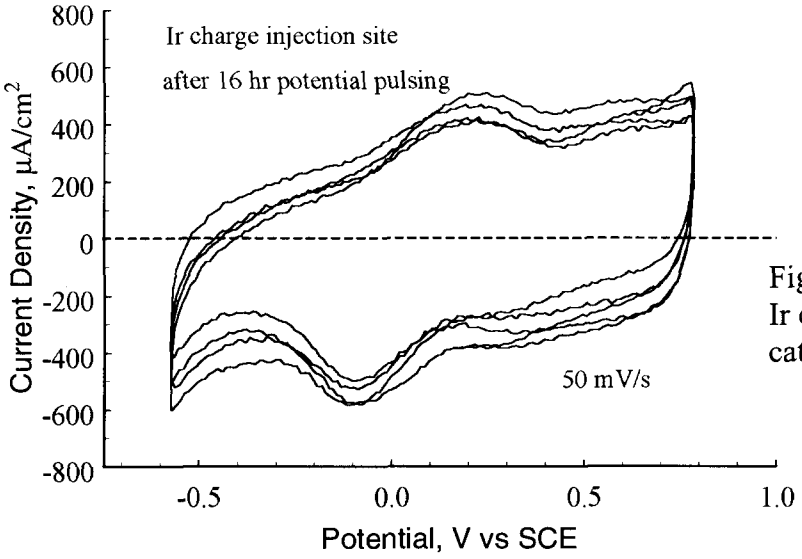

Figure 6. Cyclic voltammogram of Ir charge injection site after 16 hr cathodal pulsing at 10 mA.

Table 3. Charge injection characteristics of an activated Ir electrode site after 16 hours of continuous cathodal pulsing at 10 mA.

Time hr	E_{mc} V vs SCE	IPP V vs SCE	Access Resistance Ω	V_{oc} V vs SCE
0	0.38	0.08	72	0.08
15.5	0.32	0	68	0.08

The electrochemical characterization of the cuff electrodes was complicated by the difficulty in achieving full electrolyte access to the inner surface of the cuffs during testing. The hydrophobic inner surface allowed air to remain trapped at the electrode sites following immersion in the electrolyte. To avoid this problem, a liner of filter paper was saturated with electrolyte and placed inside the cuff. The filter paper expands slightly and wicks electrolyte to the electrode sites. This procedure significantly reduced the occurrence of high resistance sites which, prior to recognizing the problem of air occlusion at the electrode sites, had been attributed to fractured metallization.

2.3 Silicone Inner Insulation

A silicone polymer, MED-6605 with primer SP-135 from NuSil Silicone Technology (Carpartina, CA), was evaluated as a replacement for Teflon AF as the inner insulation on the cuff electrodes. The silicone is applied by spin coating and cured at room temperature. The details of the application and curing procedure are provided in Table 4.

Table 4. Application and curing procedure for MED 6605 on FEP Teflon.

Step 1.	mask charge injection sites and bonding pads with tape
Step 2.	apply NuSil SP-135 primer by spin coating at 3000 rpm for 20 s
Step 3.	cure primer by exposure to moist atmosphere (RH >50%) for 1-2 hr
Step 4.	apply NuSil MED 6605 by spin coating at 2000 rpm for 20 s
Step 5.	remove tape masks
Step 6.	cure at room temperature for 1 week

The H_2O barrier properties of MED-6605 were evaluated by leakage current measurements (details of the leakage currents measurements have been described previously in "Thin Film Hermetic Coatings ," Final Report on NINDS Contract No. N44-NS-2-2311). The leakage current response of a single layer of MED-6605 is shown in Fig. 7 at various times over a 24 day soak period in phosphate-buffered saline at 37°C. The leakage currents were quite low, $< 2 \times 10^{-12}$ A at ±5 V, and decreased to $\sim 5 \times 10^{-13}$ A after 5 days. The currents were consistently low throughout the remainder of the test period. The magnitude of the initial leakage currents for the MED 6605 were about an order of magnitude greater than those initially obtained with

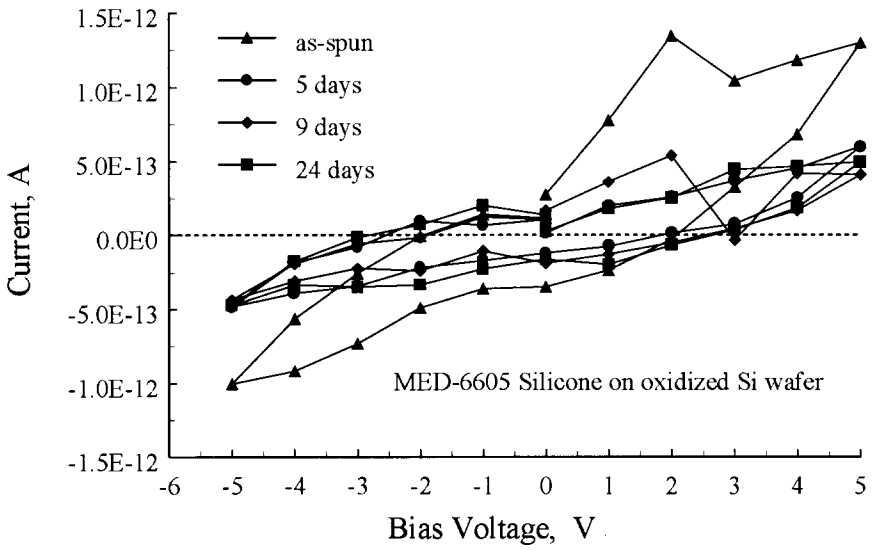

Figure 7. Leakage current response of MED-6605 silicone polymer on a thermally oxidized Si over a 24 day soak period.

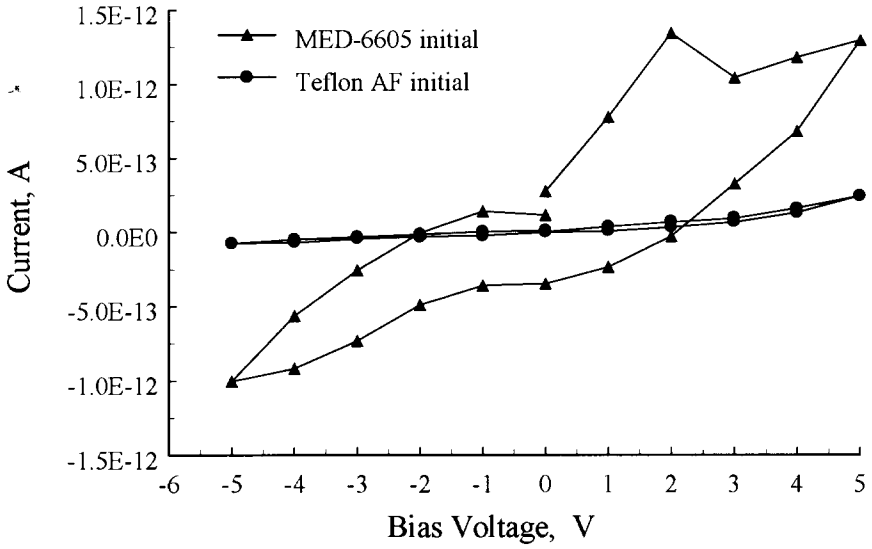

Figure 8. Comparison of initial leakage currents in PBS of MED 6605 silicone and Teflon AF on a thermally oxidized Si wafer.

Teflon AF as shown by the comparison in Fig. 8. However, the MED 6605 showed much better adhesion than the Teflon AF, surviving between 5 and 7 days without delamination from FEP Teflon or Si wafer substrates during soak tests at 90°C in PBS. Under similar soak conditions, Teflon AF delaminates with 12 hours. At 37°C, MED 6605 has remained adherent to FEP Teflon and to metallized FEP Teflon for 6 weeks without evidence of delamination.

During the course of evaluating MED 6605, several methods of improving the adhesion of the silicone and its primer to FEP Teflon were evaluated. Prior to applying the silicone, the FEP Teflon substrates were coated with amorphous silicon carbide and oxycarbide (a-SiC:H and a-SiOC:H) using the PECVD process and Ti sputtered with substrate biasing. We expected that the silicone would be more adherent to the oxide and carbide coatings than the fluoropolymer. However, there was no clear improvement in adhesion using these materials as interlayers and their use as silicone adhesion layers was discontinued. Single and multiple coats of the silicone applied at different spin rates were also evaluated. Again, no improvement in adhesion or H_2O barrier properties was apparent with multiple coats from either soak tests or leakage current measurements and the single coating was adopted for all future work.

2.4 *In vivo* Evaluation of Thin-Film Cuff Electrodes

A four-electrode cuff with the geometry shown in Fig. 1 was supplied to Hines V. A. Rehabilitation R&D Center for preliminary *in vivo* evaluation. Prior to shipping, the electrochemical behavior of each of the four electrode sites was evaluated by cyclic voltammetry. Although each site had a satisfactory response when evaluated at EIC Laboratories, all electrode sites were too resistive for charge injection when the initial *in vivo* evaluation was undertaken. At this point, we suspect that the high resistance is caused by fracture of the metallization due to excessive opening and closing of the cuff prior to testing. To avoid this problem in the future, three straightforward procedural changes have been made. These are as follows:

- attachment of the stainless steel leads to the bonding pads on the electrodes will be done at EIC Laboratories;
- *in vitro* evaluation will be limited to testing at EIC Laboratories;
- the cuff will not be unrolled except at the time of implantation.

3. CONCLUSIONS AND FUTURE WORK

In the present reporting period, the silicone polymer MED-6605 from NuSil was identified as an inner insulating layer that provides at least short-term electrode isolation during *in vitro* testing. The silicone, when used with the recommended primer, is adherent to FEP Teflon and remains so during the thermoforming operation for shaping the cuff and during subsequent soaking in PBS for 6 weeks at 37°C. In addition, with careful handling, cuffs having good electrochemical response at each charge injection site can be obtained. The major issue with electrode fabrication is now adhesion and fracture resistance of the sputtered metallization. Several

approaches to improving the mechanical properties of the metallization will be investigated in the following reporting period. Anticipated tasks for the next period include:

- evaluation of Au electroplating as a means of increasing the thickness of the metallization beyond that possible with sputtering;
- evaluation of alternative sputtering conditions to produce lower stress films, in particular to investigate higher gas pressures during Ir and Au deposition;
- fabrication and supply of four-electrode cuffs to Hines V. A. Rehabilitation R&D Center for acute *in vivo* testing in the raccoon;
- continued evaluation of the electrochemical response of thin-film Ir and activated Ir charge injection sites on FEP Teflon substrates.

4.0 REFERENCES

1. J. L. Gamble, Chemical Anatomy Physiology and Pathology of Extracellular Fluid, Harvard University Press, Massachusetts, 1954.

APPENDIX 1

Progress Report #4

Hines VA Hospital, Rehabilitation R&D Center

Progress Report #4: Thin-Film Peripheral Nerve Electrode for subcontract: *Invivo* Studies, SBIR Topic 13

Submitted to: Dr. Stuart Cogan, Head Material Sciences
EIC Laboratories, Inc.

From: James S. Walter, Ph.D.; Charles Robinson, D.Sc.; James Sweeney, Ph.D.; Jerry McLane, Ph.D.; Paul Zaszcsurynski, B.S.; Wuying Cai, M.D.; Mike Bidnar, M.D.; Talat Khan. Ph.D, Patricia Griffith, M.D.

Hines VA Hospital, Rehabilitation R&D Center, (151L) Hines, Il 60141

Introduction

The observed dexterity and control of forelimb function led us to select the raccoon as a model for graded independent muscle function. The raccoon volar forearm anatomy is described, as well as paw movements, torque and EMG responses to direct muscle stimulation using percutaneous electrodes.

We proposed that complex hand movements might be obtained with direct median nerve stimulation through an implanted multielectrode nerve cuff. Preliminary observations evaluate responses with a 12 electrode cuff implanted on the median nerve. Paw movements responses to stimulation as well as direct tendon forces were recorded.

Progress

Methods

Anatomical: The cadaver arms from three fresh and two preserved raccoons were dissected to determine the anatomy of the upper extremities concentrating on the volar forearm. Nerve branches were tagged and identified by muscle innervation.

Raccoons were observed in their cages. The use of forelimbs in feeding, digging, and grasping objects was noted. Particular attention was paid to digit movements. Responses to selective stimulation and recordings of muscles with percutaneous wires were evaluated in four animals. Raccoons (Hummel Creek Kennels, St. Louis, Missouri) weighing an average of 4.5 ± 0.26 Kg (mean ±S.E.M.) were anesthetized with 20 mg ketamine hydro-chloride/Kg and 2 mg xylazine/Kg (IM) body weight and given periodic maintenance doses for anesthesia. Ibuphronex (morphine IM) and phenobarbital (IP) were also given to reduce spasms associated with repetitive ketamine injections.

Percutaneous Stimulation Studies: Percutaneous electrodes were used for stimulation and EMG recording. The electrodes were single strands of 316 stainless steel wire insulated with a thin coating of polyamide (Life-Tech Inc. Houston Texas). For stimulating electrodes, the last 3 mm of wire was exposed. For the recording electrodes, the last 5 mm was exposed. Two stimulating electrodes were inserted in each muscle with a 27 G needle. Approximately 3 mm separated such electrodes in individual muscles. Two recording electrodes were inserted in the same muscle through a single 23 G needle. Recording electrodes were inserted approximately one cm distal to the stimulating electrodes.

Four sets of stimulating electrodes were implanted in the volar forearm lateral (L)

and distal (Di) to the insertion of the biceps muscle. The first three electrodes were inserted into superficial muscles to a depth of 3 mm after passing through the skin. These muscles were pronator teres (PT) (1 cm L), flexor carpi radialis (FCR) (1.5 cm L), and a group of muscles consisting of palmaris longus, flexor digitorium superficialis and the thumb flexor muscle (PL-FDS-TF) (3.5 cm L, 2 cm Di). The fourth set of electrodes were implanted in the deep muscle flexor digitorium profundus (FDP) (3.5 cm L, 2 cm Di and 2 cm deep). Electrodes were withdrawn and reinserted if stimulation did not produce expected paw movements. Movements to single stimulation pulses at threshold, half-maximal and maximal-stimulating currents were recorded. Several techniques were further used to help distinguish which muscles were being activated. The tendons were palpated in the forearm, the palm of the paw was held firm by an investigator so that digit flexion could be observed without wrist movement, and sustained muscle contraction to repeated stimulus pulse trains was observed.

Two sets of EMG recording electrodes were placed in the forearm muscles. The first set was placed in the muscle with the best pronation (some with primarily wrist flexion) response to stimulation. The second set was placed in the muscle with the most sensitive digit flexion. Cross talk between muscles was assessed with a third set of electrodes placed under the skin in the volar forearm in one raccoon. The EMG signals from the electrodes were observed on an oscilloscope (Gould Oscilloscope with printer, Cleveland, OH) after the signals were preamplified (Gould Universal Amplifier). Recruitment of the EMG signal was observed and plotted from the oscilloscope at increasing stimulating currents. The EMG signal was then passed through a signal artifact suppression unit (Fredrick Heir Artifact Suppression Unit, Brunswick, ME) and then into a signal rectifier and integrator unit (Gould Integrator Unit) before being displayed on a stripchart recorder. Stripchart recordings of this rectified/integrated EMG signal were then obtained with stimulating currents from threshold to maximum. Pulse trains for these strip chart recordings consisted of a 1 sec stimulation period at 20 pulses per second (pps) with the pulse duration of 100 μs. One minute recovery was given between each stimulation.

Isometric torques of the paw or digits to the one-second stimulation trains were also recorded [12]. Torque measures were obtained as the moment of force (distance times force) where the distance was 4.5 cm for all of the torque recordings. For simplification, only forces in milli-Newtons (mN) are presented (torques in units of mN·cm can be determined by multiplying by 4.5 cm). For recording wrist and digit isometric torque responses, a hinged two-plate system was used. The first plate was fixed to a rod that was anchored to the table. The forearm was then anchored to this plate with a strap. The hinge was at the level of the metacarpal-phalangeal joint for recording digit flexion and the wrist for recording flexion at this joint. The second plate was secured with tape to the distal digits or paw for these measures was connected to a force transducer (Grass Force transducer, Quincy, MA) with surgical string having minimal stretch. For pronation recordings, a plaster cast extending halfway around the forearm was taped in place. Torque measures were recorded from a rod extending out from the plaster cast and attached to the force transducer with a string. The forearm was allowed to rotate freely but was blocked from lateral movement with bars. Oil was placed on the cast to reduce any friction between the bars and cast. We also had the anesthetized animal lying on its side against its upper arm providing further stabilization. Initial conditions were optimized for each of the isometric torque measures. For wrist and digit flexion, the position was straight with slight tension. For pronation, the initial condition was supinated with slight tension.

The force transducer signals were passed through preamplifiers (Gould Universal Amplifier) and displayed on a stripchart recorder (Astromed). Wrist flexion, digit flexion, and pronation torques were recorded for the same range of stimulating currents as were

used for the EMG stripchart recordings although the range of currents used for torque measurements had a higher maximum than for EMG measurements. Force transducers were calibrated daily with free-hanging weights.

Nerve Cuff Stimulation: A twelve electrode cuff was obtained from Dr. James Sweeney, Arizona State University and a consultant on this study [1]. The cuff was composed of silastic with an inner diameter of 3 mm. Tripolar electrodes were located in each of the four quadrants with 5 mm between each electrode. The electrodes were 1 mm in diameter and were made of platinum foil embedded in silastic. The two outer electrodes of the tripolar electrodes were connected together. Positive currents were applied to the outer electrodes and negative to the inner electrodes.

In three anesthetized raccoons, the median nerve was exposed in the upper arm. The two main branches were stimulated with hook electrodes and the gross paw movements were observed. The cuff was implanted, and stimulation was conducted with 10 μs pulse durations. These short pulse durations helped us to establish a threshold current as the lowest current the stimulator could produce was 0.1 mA. Responses to longitudinal, transverse (steering) currents and combinations of longitudinal and transverse currents were evaluated. Gross paw movements to stimulation were observed. Tendons of the volar forearm were then isolated and attached to force transducers. Individual muscle responses to the different stimulating fields were then recorded.

Results

Volar Forearm Anatomy: The volar forearm consists of three muscle layers (Table 1). Going across the forearm in the ulnar direction, the superficial muscles consist of pronator teres (PT), flexor carpi radialis (FCR), palmaris longus (PL), a muscle we named thumb flexor (TF) and flexor carpi ulnaris (FCU). The PT and FCR have the same origin and attachments in the raccoon as in the human. The TF tendon originates on the medial epicondyle, goes deep in the forearm, joins the FDP tendon sheet in the wrist area and splits from the FDP to attach to the thumb phalanges. The PL originates from the medial epicondyle and the bulk of this muscle forms a multiheaded attachment to the palm fascia. The FCU in the raccoon has origins on the medial epicondyle and olecranon. The FCU contains a pisiform bone and inserts on the ulnar metacarpal. Flexor digitorium superficialis (FDS) is in the second muscle layer. This muscle divides into four tendons which then come to form an adherent sheet in the wrist area with no apparent separate tendon motion possible. The FDS tendons then divide again into four separate tendons in the palm. These tendons along with the FDP tendons pass under a digital pulleys array as they go to their phalangeal attachments. FDP is in the third layer. It also forms separate tendons in the distal forearm, a thick tendon sheet in the wrist, and again splits into individual tendons in the palm. The fibrous attachments of the different tendon groups in the wrist such as TF, PL, FDS and FDP negated separate thumb and digit flexion from the forearm. Arising from the FDP palmar tendon sheet in the palm is a sheet of muscle which then extends upwards along the borders of the digits similar to the lumbricles in humans. The deepest muscle in the distal forearm is the pronator quadratus (PQ). It is thin and extends from the distal third of the ulna to the distal third of the radius. The palm in these adult animals were approximately 2.5 X 2.5 cm and 1 cm thick. The digits extend out an additional 3 cm and are easily distinguishable. The palm is well developed with thenar, hypothenar, and interosseous muscles.

Four large nerves are identifiable in the raccoon upper arm: radial, ulnar, and two branches of the median nerve. These were named superficial (S) and deep (D) median nerve branches. The deep branch of the median nerve passed under a bony bridge in the

humerus before entering the volar forearm. The bony bridge is believed to be a calcified bicipital aponeurosis. In the forearm, after innervation was given to PT, PL, TF, FCR, FDS, FDP, and occasionally a small FCU branch, the two median nerve cords combined to form a unified nerve which became immersed with the FDS tendons as it traveled to the radial three digits of the hand. The ulnar nerve traveled around the medial epicodyle then gave off an FCU branch, a FDP branch, intrinsic hand muscle innervation, and then innervated the ulnar two digits of the finger. The radial nerve was also identified in the upper extremity and travelled to the forearm extensors.

Table 1. Anatomy of the Raccoon Volar Forearm Innervated by the Median Nerve

Muscle	Origin	Insertion	Action	Innervation
Superficial Muscles				
Pronator Teres (PT)	medial epicondyle	proximal radius	forearm pronation of arm	Median S
flexor carpi radialis (FCR)	medial epicondyle	2nd metacarpal	wrist flexion	Median S
Palmaris Longus (PL)	medial epicondyle	multiple heads palmar fascia	palm fascia retraction	Median S
Thumb Flexor (TF)	medial epicondyle	thumb phalanges	thumb flexion	Median D
Flexor Carpi Ulnaris (FCU)	medial epicondyle olecranon	fifth metacarpal, pisiform	wrist flexion ulnar deviation	Ulnar Median S
Second Layer				
Flexor digitorium Superficialis (FDS)	medial epicondyle	phalanx of digits radius, ulna	flexion of fingers	Median D
Third Layer				
Flexor Digitorium Profundus (FDP)	upper anterior radius and ulna	phalanx of digits four digits	flexion of fingers	Median D Ulnar
Pronator Quadratus (PQ)	radius and ulna	radius and ulna	pronation of forearm	Median S & D
Palm Muscles				
Hypothenar	carpal bones	ulnar digit metacarpal, phalanges	flexes little finger opposition abduction	Ulnar
Thenar	carpal bones	thumb metacarpal, phalanges	flexes thumb opposition abduction	Median S & D Ulnar

Muscle	Origin	Insertion	Action	Innervation
Interosseus	between metacarpals	phalanges	adduction, abduction	Ulnar
Lumbricals	FDP	phalanges	finger flexion	Ulnar

Functional Observations to Direct Muscle Stimulation with Percutaneous Electrodes: The raccoons were observed as they ranged about in their cages and ate. None of the raccoons demonstrated active opposition of the ulnar digits and thumb to hold food or a bar. A type of passive opposition occurred, however, with spreading of the digits over a bar while standing on it. The thumb is small and had little functional use. When the animals climb and hang from a bar, the paw is used like a claw and hooks over the bar. Clawing actions of the paw are also seen using the strong flexor muscles of the forearm when they dig in the cage bedding for food. They hold food between their two forepaws much like a squirrel. Thus, little individual digit function was noted. Because the function of the paw of the raccoon was more like a claw than the dextrous fingers of the human, further studies of torque and EMG were limited. We primarily observed three movements of the paw to volar forearm muscle contraction: pronation of the forearm, wrist flexion and digit flexion. The digits acted in unison so torque studies were conducted with the digits taped and strapped to a single force plate.

Stimulation of intrinsic paw muscles resulted in selective movement of digits. However, due to their small size, intrinsic paw muscles were not suitable for simultaneous stimulation and EMG recording, and they were not further studied. Volar forearm muscles were implanted with stimulating electrodes, and results from two of the animals are presented here. Four sets of muscles or muscle groups, as defined in the Materials and Methods section, were stimulated. Selective responses to stimulation were typically seen at threshold currents ranging from 0.2 to 1.5 mA. PT induced pronation and some wrist flexion; FCR induced wrist flexion, and pronation. The PL-TF-FDS group induced primarily flexion of all of the digits with some wrist flexion, and FDP induced digit flexion responses indistinguishable from the PL-TF-FDS group.

At half maximal currents, 0.4 to 4 mA, there was increased pronation, wrist, and digit flexion observed with less selectivity of movement to stimulation. Maximum currents, 0.6 to 8 mA, continued to increase magnitude of motions and decrease selectivity of motions. However, increased digit flexion and some elbow flexion was invariably seen indicating recruitment of some of the major flexor muscles of the forearm.

EMG and Torque Responses to Percutaneous Stimulation: Volar forearm EMG and torque responses were recorded from two of the four groups of stimulating electrodes, the two sets that showed the greatest difference in forearm movement. In most of the studies this consisted of the PT set of electrodes and the PL-TF-FDS group of muscles.

Stimulation of each muscle or muscle group resulted in a biphasic M wave EMG response of short latency (Fig. 1A). The M waves were electronically modified to display the average EMG evoked voltage on a stripchart recorder. Artifact suppression and rectification is shown in Figure 1B and a typical strip chart recording of the integrated EMG response is shown in Figure 1C. This allowed for the simultaneous recording on the strip chart of EMG and torque measures. Long-latency F waves were only recorded in one animal. These waves had a 90 ms delay and were much smaller in amplitude than the M waves.

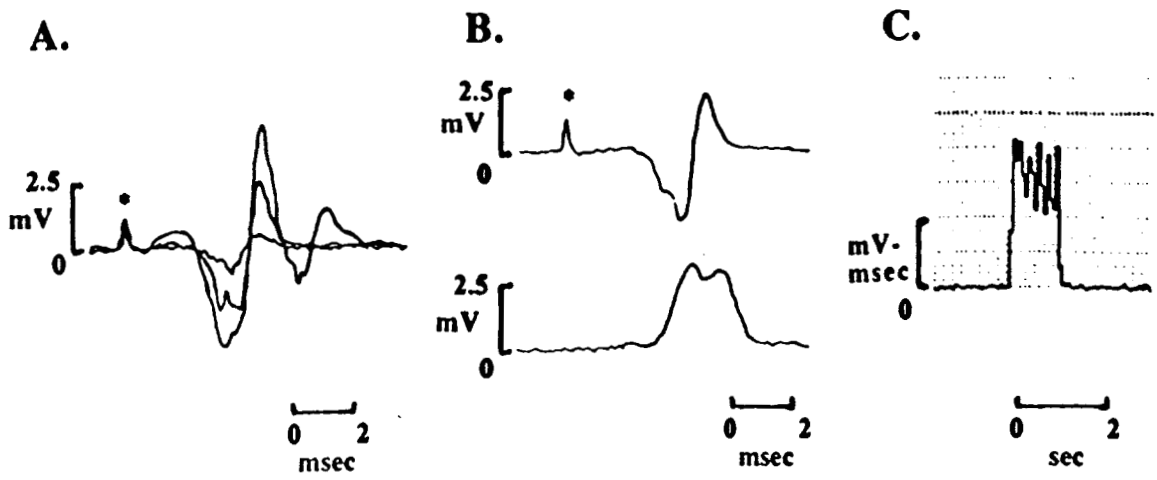

Fig. 1. Percutaneous stimulation and recording of EMG activity from FCR. **A.** Biphasic M waves including stimulation artifact for threshold, 1/2-maximal, and maximal stimulating current. **B.** Top waveform is biphasic M wave including stimulation artifact and bottom waveform is rectified with artifact suppression. **C.** Stripchart recording of integrated M wave as shown in lower record of B from 100 μsec pulses at 20 pulses per second (pps) for one second.

In conjunction with recording the EMG responses to stimulation, isometric torque recordings from the paw were obtained. Recordings were reproducibly obtained for finger flexion, wrist flexion and forearm pronation. After stimulation, torque forces returned to prestimulation levels. For pronation recordings, several trials were usually required to obtain reproducible results with no apparent lateral movement. Figure 2 shows combined EMG and wrist torque responses to the PL-FDS-TF muscle group stimulation. These records were obtained with the 1 sec stimulation at 20 pps, and both EMG and torque show abrupt onsets that are maintained throughout the 1 sec of stimulation. Both measures also increase in response to increasing current strengths.

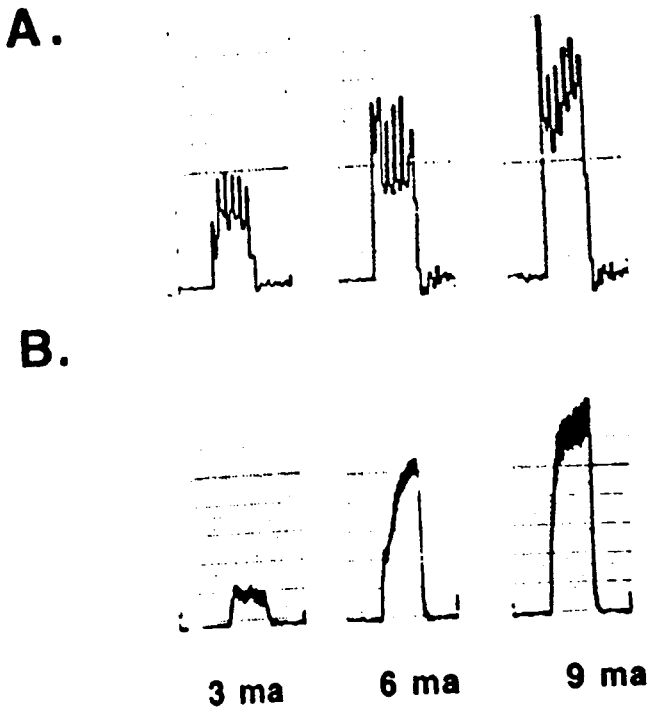

Fig.2. **A.** EMG of stimulated PL-FDS-TF group. **B.** Wrist flexion torques for 3-, 6-, and 9 mA stimulating current at 20 pps for one second, 100 μsec pulse duration.

Good selectivity of muscle stimulation was observed based on EMG measures (Fig. 3). At the threshold and higher currents, PT stimulation recruited increased EMG response from the PT muscle with little EMG response from FDP (Fig.3A). Similar selectivity was observed with FDP stimulation (Fig 3B). For the four animals investigated, selectivity based on EMG recordings was seen. At 50% recruitment in the EMG signal of the stimulated PT the average recruitment in FDP was 8.5 ± 13.9 mV·ms (mean $\pm$ S.D. At 50% recruitment in the EMG signal of the stimulated FDP the average recruitment in PT was 10.8 ± 9.0 mV·ms. Selectivity of muscle stimulation is thus shown based on EMG recordings from the muscles.

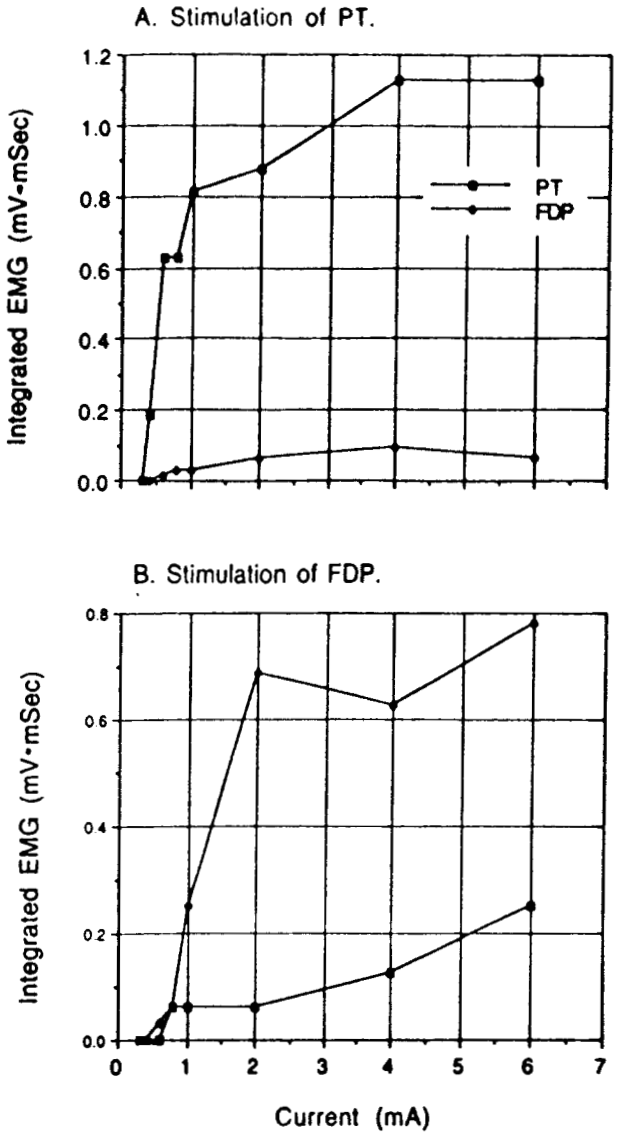

Fig. 3. **A.** Peak EMG responses of PT and FDP to PT stimulation. **B.** Responses to FDP stimulation. Records from one raccoon.

Good selectivity of muscle stimulation was also obtained based on isometric force (torque) recordings (Fig. 4). At the threshold and higher currents, PT stimulation resulted in higher pronation forces (Fig. 4A) with little wrist or digit force (Fig. 4B, C). Similarly, at the threshold and higher currents, FDP stimulation resulted in increased wrist and digit flexion forces. Because of some difficulties in initial experiments in obtaining pronation torques without lateral movement, adequate force (torque) records were obtained in the last two animals. One of the animals is represented in Figure 4 and the second animal gave similar results.

Motion Responses to Stimulation with Bipolar Hook Electrode and Multi-Electrode Cuff

Considerable effort was needed to identify, isolate and stimulate the two cords of the median nerve containing motor fibers. These two branches had to be distinguished from a sensory median nerve branch as well as the ulnar nerve. The surgery is complicated by the vascular bed around these various branches.

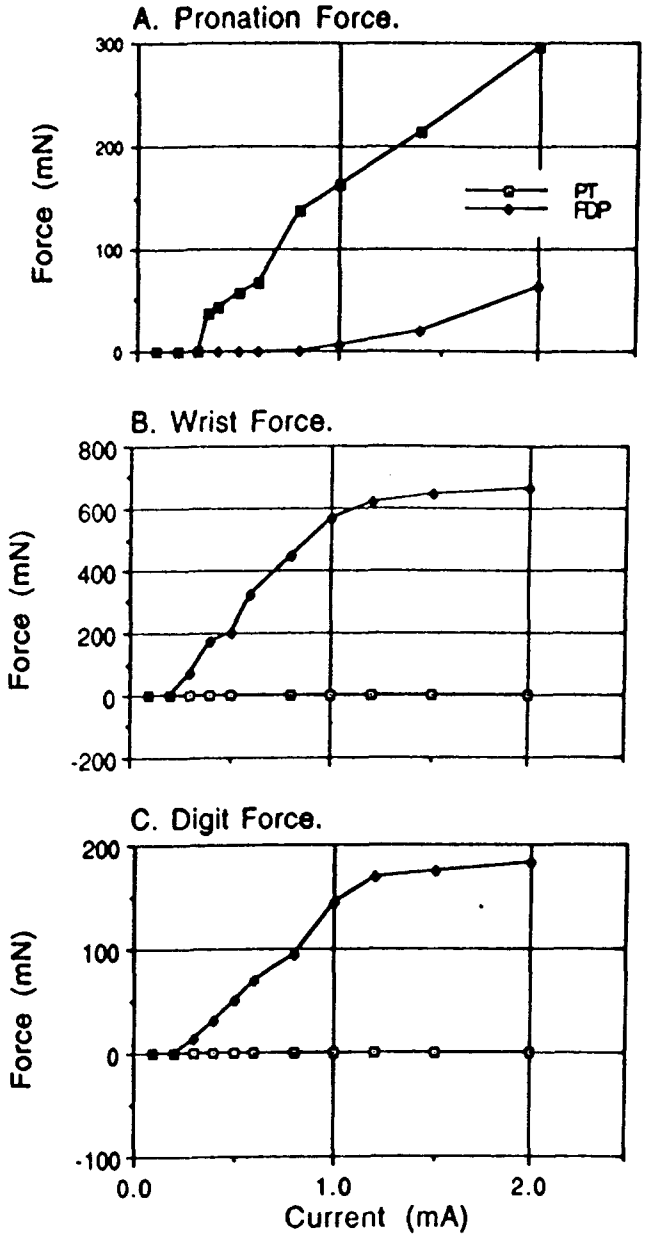

Fig 4. Force responses for PT and FDP stimulation with percutaneous electrodes. **A.** Pronation, **B.** Wrist, and **C.** Digits.

For three raccoons, we were careful with our isolation of the nerves. Using the bipolar hook electrodes, the animal showed selective responses to stimulation. The superficial and deep median nerve branches in the upper arm were stimulated individually. Threshold, half maximal and maximal stimulating currents resulted in increased number of paw movements for one animnal are shown in Table 2. Stimulation of the superficial branch primarily induced pronation. Stimulation of the deep branch of the median nerve

primarily induced wrist and digit flexion.

The 12 electrode cuff was then placed around the two branches of the median nerve. As shown in Figure 5, 0° & 270° locations of tripolar electrodes were closest to the superficial branch. 90°, 180° locations were closest to the deep median nerve trunk. A suture was placed around the cuff to prevent movement and keep it snug against the two trunks of the median nerve. The tripolar electrodes were first evaluated. The most pronation was seen at the 0° angle which was primarily over the superficial branch. The angles of 90°, 180° primarily resulted in elbow flexion. At 270° wrist and digit flexion was observed at increasing stimulation currents. Transverse currents also showed selectivity. Combining the longitudinal current with a maximal steering (transverse) current had an effect on the recruitment curve. The threshold currents were changed and the recruitment curve was over a wider range of currents (Table 2). However, observed gross movements of the paw were little changed with the addition of steering currents.

Table 2. Paw movements to stimulation of the median nerve branches with a bipolar hook electrode and with the cuff electrode.

	threshold (mA)	1/2 Max (mA)	Max. (mA)
Bipolar Hook Electrode[a]			
Superficial Branch	pro (0.5 to 0.8)	pro & elb (1.5)	pro & elb (2.0 to 3.0)
Deep Branch	dig & wri (0.3)	dig & wri (0.6)	dig & wri (0.6)
Cuff Electrode			
Tripolar 0°[a]	pro (0.4)	pro (0.7)	pro & elb (1.3)
Tripolar 90°	elb (0.3)	elb (0.7)	elb (1.1)
Tripolar 180°	elb (0.8)	elb (1.1)	elb (1.5)
Tripolar 270°	wri & dig (0.3)	wri & dig (1.0)	wri & dig (1.5)
transverse 0°[b]	pro (1.0)	pro (2.5)	pro & elb & wri (5.0)
Transverse 90°	elb (0.6)	elb (1.1)	elb (1.5)
Transverse 180°	pro (3.0)	elb & pro (4.5)	elb & pro (6.0)
Transverse 270°	dig wri & elb (1.5)	dig wri, & elb (3.0)	dig wri, & elb (5.0)
Tripolar with steering 0°[c]	pro (0.1)	pro (0.6)	pro & elb & wri (1.4)
Tripolar and steering 90°	elb (0.1)	elb (0.5)	elb (1.0)
Tripolar and steering 180°	elb (0.4)	elb (0.8)	elb (1.1)
Tripolar and steering 270°	wri & dig (0.2)	wri & dig (0.5)	wri & dig (1.1)

[a] pro - pronation, elb - elbow flexion, wri - wrist flexion, dig - digit flexion, currents in volts. Stimulation applied with for 10 μs pulses applied singly and in trains of 20 pps for 1 sec.

[b] transverse current applied with the negative electrode only to the center electrode of a tripolar at the angle stated and the positive electrode to a single electrode on the opposite side of the cuff.

[c] tripolar with steering current. A transverse current is named a steering current when applied with a longitudinal electrode. The steering current was applied just below threshold (this current was established during the threshold determination of the transverse current).

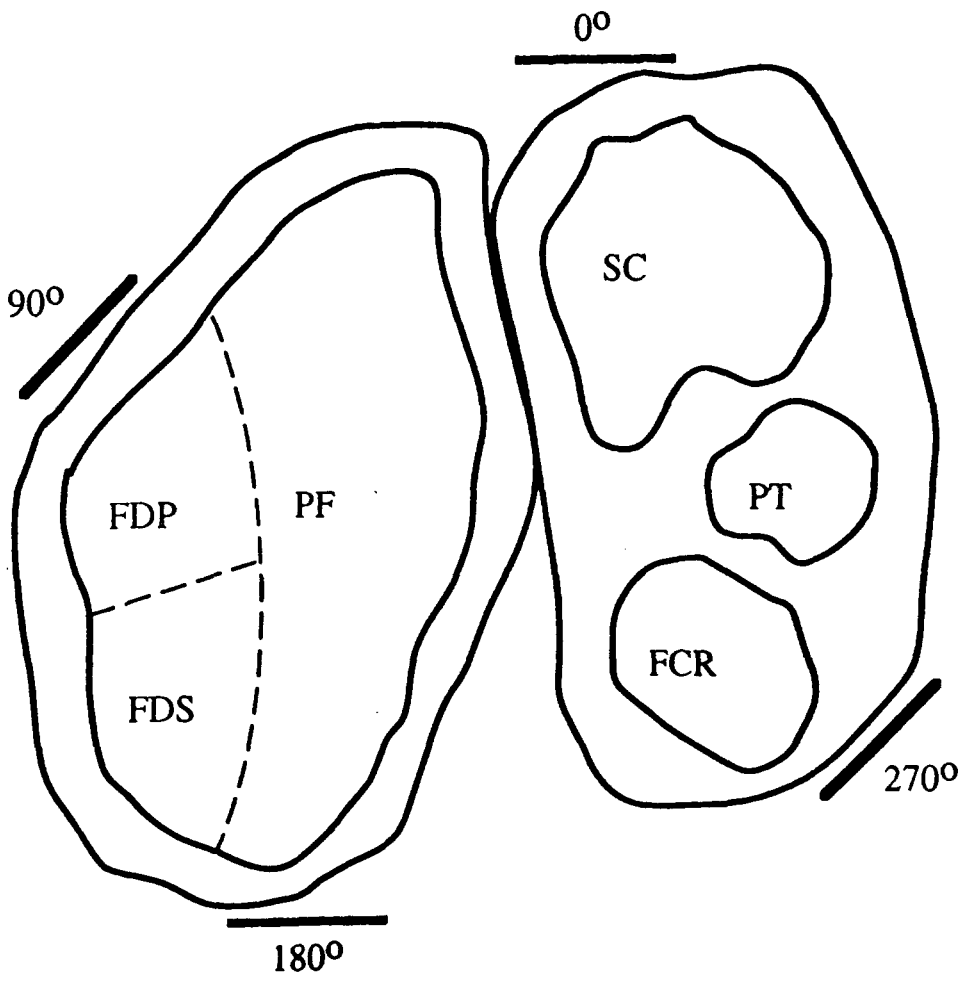

Fig. 5. Median nerve fascicles in relation to the tripolar electrodes. A tripolar electrode is located longitudinaly along the nerve at each of the positions indicated.

Tendon Forces to Stimulation with the Median Nerve Cuff Electrode : The muscles of the volar forearm were isolated and connected to force transducers. The upper and lower arms were blocked with rods to prevent movement. Tripolar electrodes were first evaluated. The most separation of tendon forces were seen at the 0^{o} position which was primarily over the superficial branch of the median nerve (Fig. 6A). At this position and at 0.5 to 1.0 mA stimulating current PT and FCR show strong recruitment with other muscles not recruited. At the other angles, 270^{o} a similar pattern is shown with the early recruitment of FDP and PL. The recruitment pattern is consistent with the locations of the nerve fascicles in relation to the electrodes Fig. 5. Figure 7 also shows this pattern for recruitment of the muscles at each of the quadrants. FDS is primarily recruited at 90^{o} and 180^{o}. FCR is recruited primarily at 0^{o} and 90^{o}. However, strong recruitment is shown at 0 and 180^{o}. PT shows early recruitment at 90^{o}. PL showed little selection of recruitment based on the location of the tripolar electrode. It is not clear how PL produced such strong forces as it is a small muscle. WE are further evaluating the anatomy of PL. For FDP, a

complete record was not obtained but strong recruitment is shown at 0- and 180°.

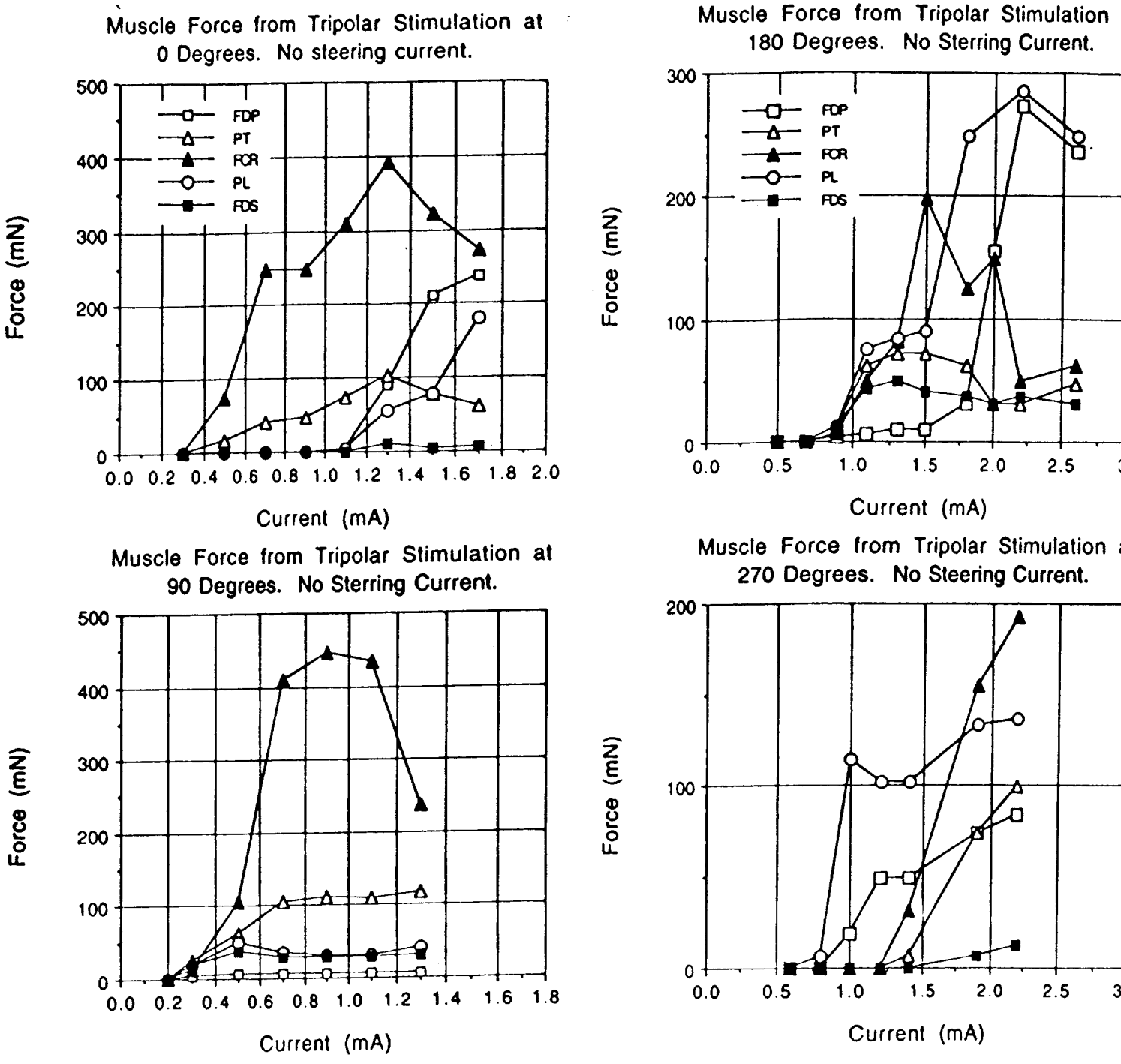

Fig 6. Tendon force responses to longitudinal current stimulation at 0°, 90°, 180°, 360°.

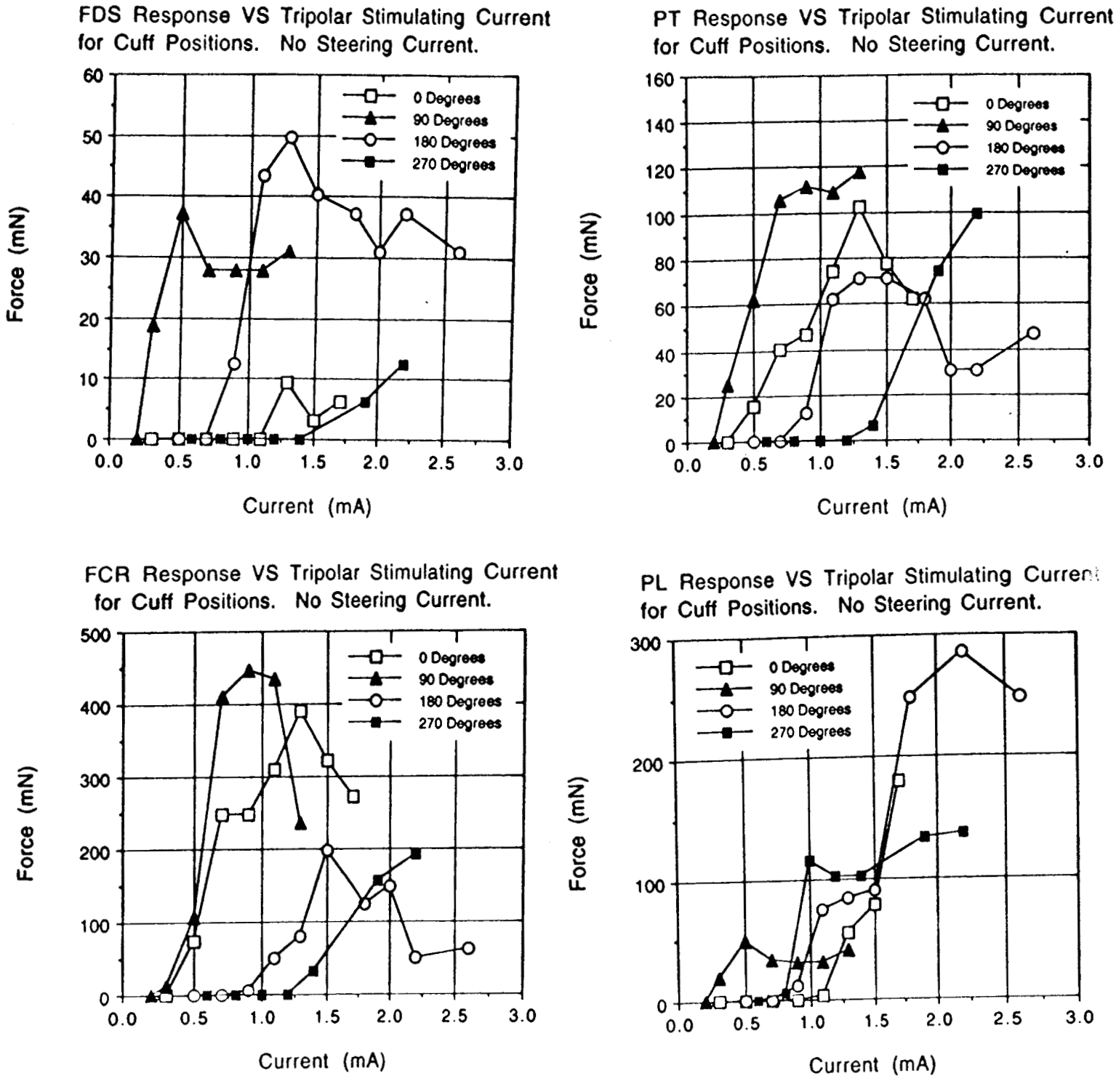

Figure 7. Recruitment patterns of individual muscles for each of the longitudinal electrodes of 0°, 90°, 180°, 360°.

Applying steering currents at the same time as the longitudinal currents resulted in much lower threshold currents longitudinal currents alone. The steering current was applied just below threshold based on transverse currents being applied alone. At 0^{O} PT and FC were recruited first. At 90^{O} FC showed a strong recruitment curve. At 180^{O} PL was again strongly recruited. At 270^{O} PL and FDP were strongly recruited.

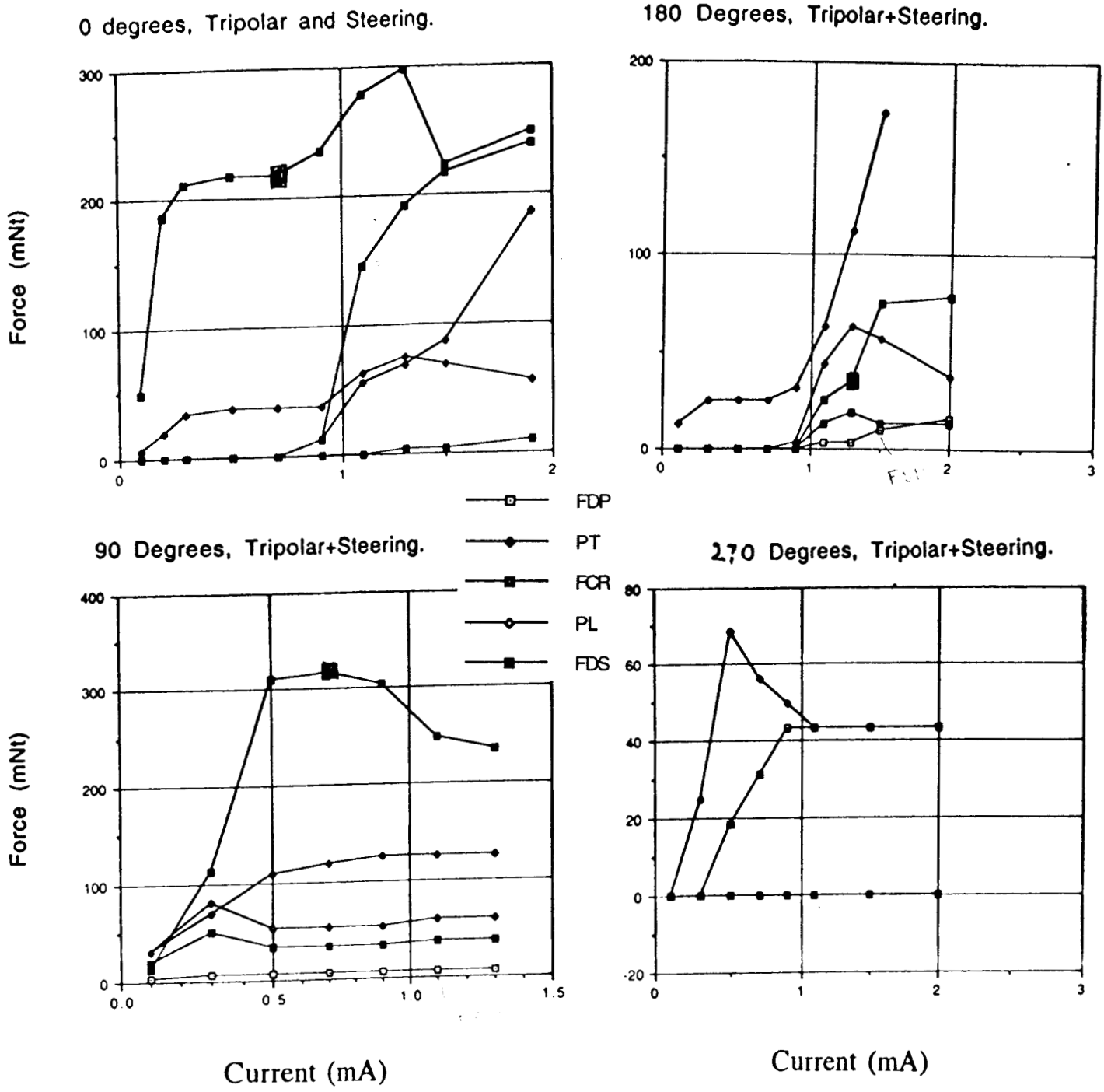

Fig 8. Recruitment force to longitudinal currents with a steering current just below threshold as determined from transverse electrode stimulation studies.

Discussion

The raccoon appears to be a suitably large laboratory animal for the evaluation of upper limb neuroprosthetics. They are relatively disease free and available from reputable vendors that breed animals for research and furriers. Experiments in these animals can only be conducted under anesthesia, but the use of squeeze cages allows for easy injection of anesthetic. Their relatively large paws allow for observation of both paw and digit motions even when the animals are moving about in their cages.

The muscles of the forearm are similar to the humans but with some similarities to lower animals such as cats [4,9,15,16]. Major digit flexors such as FDS, FDP, and intrinsic muscles of the hand have the same functions in humans and raccoons. In the cat one sees multiple origins of the FCU, and in the raccoon there are still multiple origins, while in humans there are two origins. In all three species the primary origins are on the medial epicondyle and the olecranon. The thumb flexor muscle is unique to the raccoon and is a possible precursor to the FPL.

There are some important limitations of this animal as a model for upper limb neuroprosthetics. In contrast to the human with a single median nerve cord in the upper arm, the median nerve cords in the raccoon appear not to combine in the brachial plexus area but combine after forearm innervation is given [4, 9]. This median nerve arrangement might provide improved selectivity because anatomically separated branches may be easier to selectively stimulate.

The separate tendons that are bound together at the wrist and then separate in the palm appear to be an early variant on tendon sheaths. In no raccoon were digit tendons individually gliding. This binding of the tendons resulted in movement of all of the digits together which probably serves clawing and digging functions. This also duplicates function in cases of injury. This is quite distinct from humans where individual digit movement is predominant. Also the FDS and FDP tendons adhere to each other as they pass through annular ligaments in the fingers. Separate FDS, FDP insertions were not identifiable even in fresh dissection. This may be another evolutionary aspect which later evolved into separate functions. Insertions in the digits were also different in this animal. The digit flexion observations did not show separate distal interphalangeal (DIP) flexion from proximal interphalangeal (PIP) joint flexion. The raccoon has a thick palm and digit pads covering the volar paw which obscure digit fine movements. Finger flexors cross the wrist, and flexion of fingers results in flexion forces across the wrist.

Another major difference from the primate hand is seen in the small thumb of the raccoon with limited function. Passive but not active opposition with the thumb was observed in this animal. There was also some individual raccoon variants in anatomy. The small number of raccoons being studied made it difficult to generalize incidence of specific findings to the raccoon species. One raccoon showed a median nerve branch to the FCU. The amount of FDS and FDP inter-tendon attachment at the wrist prior to splitting back into separate tendons varied.

Separate graded responses to intramuscular stimulation were obtained with three independent measures: visual observations of movements, EMG and torques. These measures indicate that basic paw movements can be reproduced with electrical stimulation. The stimulation and recording techniques shown here are suitable for further neuroprosthetic studies.

The preliminary cuff studies show that selective responses can be obtained [17]. The selectivity was shown both with observations of paw movements and with recording tendon forces of individual muscles. Longitudinal currents produced recruitment responses. The addition of steering currents resulted in modes changes in responses. However, thresholds for longitudinal currents were dramatically reduced with steering

currents.

The preliminary results using the cuff also show some limitations. The cuff must be carefully implanted. The divided median nerve is a major limitation of the model but does allow for stimulation of the the cords individually before implanting the cuff.

This animal model may be suitable for the development of some upper limb neuroprosthetic applications including the development of cuff electrodes, feedback control and sensors. All these applications would benefit from the availability of an animal model and stimulation protocols providing selective and graded responses [2,6,10]. No other nonprimate animal model allows for such extensive evaluation of hand movements. However, cited limitations of this animal model will need to be taken into consideration.

References

1. Sweeney J.D., Crawford, N.R.and Brandon, T.A. Neuromuscular stimulation selectivity of multiple-contact nerve cuff electrode arrays. Medican & Bilogical Engineering & Computing. In Press.
2. Handa, Y., Hoshimiya, N. Functional electrical stimulation for the control of the upper extremities. Med. Prog. through Technology 12:51-63, 1987.
3. Gorman P.H. and Mortimer, J.T. The effect of stimulus parameters on the recruitment characteristics of direct nerve stimulation. IEEE Trans. Biomed. Engin. 30:7, 1983.
4. Jabaley, M.E., Wallace, W.H., Heckler, F.R. Internal topography of major nerves of the forearm and hand: A current view. J. Hand Surgery 20:1-18, 1993.
5. An Kai-Nan, A., Berglund, L., Cooney, W.P., Chao, E.Y. and Kovacevic, N. Direct *in vivo* tendon force measurement system. J. Biomechanics, Vol. 23, No. 12. 1269-1271, 1990.
6. Keith, M.W., Peckham, P.H., Goeffrey B, Thorpe, B.S. et.al. Implantable functional neuromuscular stimulation in the tetrapelic hand. J. Hand Surgery 14A:524-530, 1989.
7. Ketchum L.D., Tompson D., Pocick, G., Wallingford, D. A clinical study of forces generated by the intrinsic muscles of the index finger and the extrinsic flexor and extensor muscles of the hand. The Jounal of Hand Surgery, Vol. 3., No. 6, 1978.
8. McKinley, J.C. The intraneural plexus of fasciculi and fibers in the sciatic nerve". Arch. Neurol. & Psychi., 6: 377, 1921.
9. Pansky, B., House, E.L.: Review of Gross Anatomy. Macmillan Publishing Co., NY, 5th Ed. pp.585, 1984.
10. Peckham, P.H., Keith, M.W. and Freehafer, A.A. Restoration of functional control by electrical stimulation in the upper extremity of the quadraplegic patient. J. Bone Joint Surg. 70A:144-148, 1988.
11. Rushton, W.A.H. "The effect upon the threshold for nervous excitation of the length of nerve exposed, and the angle between current and nerve," J. Physiol., vol. 63, pp. 357-377, 1927.
12. Schuind, F., Garcia-Elias, M., Cooney, W.P. III, An, K.: Flexor tendon forces: *In vivo* measurements. J. Hand Surg., 17:291-298, 1992.
13. Smith, B. Peckham, P.H., Keith, M.W., Roscoe, D.D. An externally powered, multichannel, implantable stimulator for versatile control of paralyzed muscle. Trans. Biomed. Eng. 34:499-509, 1987.
14. Sunderland, S. "The intraneural topography of the radial, median, and ulnar nerves". Brain, 68:243-298, 1945.
15. Sunderland, S. and Ray, L.J. "The intraneural topography of the sciatic nerve and its popliteal divisions in man". Brain, 71:242, 1948.
16. Sunderland, S. "Nerves and Nerve Injuries". Churchill Livingstone, NY., NY., p. 36, 1978.
17. Sweeney J.D., Ksienski D.A., Mortimer, J.T. A nerve cuff technique for selective excitation of peripheral nerve trunk regions. IEEE Trans. Biomed. Engin. 37:706-715, 1990.